Transient internal wave excitation of resonant modes in a density staircase

Joel Bracamontes-Ramirez[1,*] and Bruce R. Sutherland[2]
[1] *Institute of Environmental Physics*
University of Bremen, Bremen, Germany
[2] *Departments of Physics and of Earth & Atmospheric Sciences*
University of Alberta, Edmonton, AB, Canada T6G 2E1

(Dated: November 5, 2023)

Abstract

The density of the ocean generally increases continuously with depth as a consequence of variations in salinity and temperature. In some regions, however, the density profile of the ocean adopts a (double diffusive) staircase structure in which successive layers of uniform density fluid are separated by rapid density jumps. Previous work has theoretically examined the transmission and reflection of periodic internal (gravity) waves incident upon a density staircase. This predicted the existence of transmission spikes (global modes) for certain combinations of frequency and horizontal wavenumber in which the incident waves transmit perfectly across a density staircase. It was hypothesized that the transmission spikes occur when the incident waves resonate with natural modes of disturbances in the staircase. Here we derive theory to investigate the interactions between incident internal waves and modes. We demonstrate a close correspondence between the frequency for incident waves at a transmission spike and the real-part of the frequency of modes at the same horizontal wavenumber. However the frequency of the corresponding modes have negative imaginary part corresponding to exponential decay of the modes in time. We perform numerical simulations to examine the impact of this near-resonant coupling when a vertically localized, quasi-monochromatic internal wave packet interacts with a density staircase. In a range of simulations with fixed incident wave frequency and varying horizontal wavenumber, the measured transmission coefficient does not exhibit transmission spikes, but decreases monotonically with increasing horizontal wavenumber about the critical wavenumber separating strong and weak transmission. We show this occurs because the incident wave excites modes that then slowly transmit energy above and below the staircase at a rate consistent with the predicted decay rate of the modes. This rate is slower for staircases with more steps with the decay time increasing as the cube of the number of steps.

Keywords: interfacial waves; density staircase; transmission; wave tunneling

I. INTRODUCTION

Internal (gravity) waves propagate in density-stratified fluids, transporting energy both horizontally and vertically. Particularly in the ocean they play an essential role in the vertical

* joelbra.92@gmail.com

transport of heat and salinity caused by the mixing that occurs when the waves break [1]. The frequency of propagating internal waves is limited by the background buoyancy frequency, which is a measure of rate at which the background density increases with depth. In particular, vertically propagating internal waves reflect from weak stratification where the buoyancy frequency is less than the incident wave frequency, though the waves give rise to an evanescent disturbance in the weakly stratified region (e.g. see Sutherland [2]). Of particular interest is the interaction between downward propagating internal waves incident upon a thermohaline density staircase. The vertical profile of density in a staircase is characterized by steps of uniform density separated by sharp density jumps, which have been observed in different regions of the ocean from the tropics to the Arctic Ocean, occurring as a result of double diffusive processes [3–8]. Within the steps of the staircase, an incident internal wave is evanescent. However, if the steps are sufficiently small compared to the scale of the incident wave, the wave can partially transmit across the staircase [9, 10]. This tunnelling phenomena has also been explored in the context of wave propagation across staircases occurring in giant planets [11].

Of particular interest is the interaction between internal waves and the thermohaline staircase in the Arctic Ocean. As Arctic sea ice cover decreases due to global warming, winds blowing over the exposed ocean surface or driving mobile ice floes can more frequently generate internal waves that then propagate downward and interact with a thermohaline staircase [12]. Observations have revealed the robust presence of a staircase spanning horizontally over a thousand square kilometers in the Canadian Basin, being situated a few hundred meters below the surface and extending over 100 m depth [13, 14]. The steps of the staircase have depths on the order of 1 m with sharp density jumps having thickness on the order of 1 cm. Should incident downward propagating internal waves partially transmit through the staircase they can act as a source of mixing that may bring warm and salty Atlantic water at depth closer to the surface, which may then enhance sea ice melting.

Theoretical predictions have been made for the transmission and reflection of monochromatic (in frequency) horizontally periodic internal waves incident upon a single uniform-density slab of fluid [15] and two mixed layers [16]. This work was extended to examine the influence of shear across a single step [17, 18] and allowing for the incident wave to be manifest as a horizontally localized beam [19, 20]. More recently, an analytic prediction was developed for transmission of an incident plane wave across a density staircase with an arbitrary number of equal-sized steps [9]. The work included consideration of background rotation and presented numerical solutions for transmission across unequal steps. In all cases the work predicted a sharp transition between weak and strong transmission at a critical incident wave frequency, which is proportional to the horizontal wavenumber for hydrostatic waves. Waves with moderately larger frequency than this critical value exhibited a sequence of transmission spikes for which the incident waves entirely transmitted without reflecting. The number of transmission spikes corresponded to the number of steps in the staircase. It was suggested that these transmission spikes occurred as a consequence of the incident waves resonating with natural oscillating modes of the staircase, a phenomena examined in theoretical detail here.

In all the above theoretical studies the incident waves were assumed to have a single frequency, steadily impinging upon single or multiple density steps. In reality, internal waves are transiently generated and so are manifest as a wavepacket. The interaction between a wavepacket and density steps has not been well studied, except for a numerical examination of finite-amplitude effects associated with a wavepacket propagating across a density step with no density jump above and below the step [21]. In the theoretical-numerical work presented here, we examine the transmission resulting from the transient interaction between a incident vertically localized internal wave packet and a density staircase. We demonstrate that transmission spikes do not occur in this case because the incident wave packet puts energy into modes that then slowly re-radiate this energy both above and below the staircase. This effect is stronger for a staircase with more steps.

In Section II, we review the theory of plane wave transmission across a density staircase [9] for the specific case of no background rotation. We also derive an expression that gives the dispersion relation of natural modes of the staircase, and we consider the near-resonant excitation of these modes forced transiently by an incident wave packet. Section III describes the numerical model and diagnostics applied to characterize the time evolution of energy above, below and within the staircase. The simulation results and their comparison with theory are presented in Section IV. Concluding remarks and application to the thermohaline staircase in the Arctic Ocean are considered in Section V.

II. THEORY

Here we consider the vertical structure of horizontally periodic disturbances associated with a density case having J equal steps bounded above and below by uniformly stratified fluid. The fluid is assumed to be inviscid and Boussinesq, and the disturbances are assumed to be small-amplitude and two-dimensional with structure in the x-z plane, with x horizontal and z vertical. For simplicity, the influence of background rotation is ignored.

First we describe the layout of the problem, describing the background density profile of the staircase, and giving general solutions for the vertical structure of disturbances in the staircase. We then specifically review the theory of internal wave tunneling across a staircase that predicts the transmission coefficient as it depends upon the horizontal wavenumber and frequency of the incident wave. From this prediction we derive the methodology to determine numerically the dispersion relation for "global modes" for which there is pure transmission at non-zero horizontal wavenumber. We then consider the natural modes of the density staircase, giving an expression from which the dispersion relation of vertical modes can be derived. Showing that the global modes and natural modes are near-resonant, we examine the excitation of the natural modes that are transiently forced by incident waves with wavenumber and frequency near that of the global modes.

A. Problem setup

In setting up the density profile for the staircase, we imagine the fluid in the absence of a staircase is uniformly stratified with constant buoyancy frequency N_0. We now suppose that this profile is uniformly mixed across J steps, each of depth L, with the staircase extending between $z = 0$ and $z = -JL$. The corresponding background density profile is thus given by

$$\bar{\rho}(z) = \begin{cases} \rho_0 \left(1 - \frac{\Delta\rho}{\rho_0}\frac{z}{L}\right), & z > 0 \\ \rho_0 \left(1 + \left(j - \frac{1}{2}\right)\frac{\Delta\rho}{\rho_0}\right), & -jL < z < -(j-1)L, \quad j = 1, 2, \ldots, J \\ \rho_0 \left(1 - \frac{\Delta\rho}{\rho_0}\frac{z}{L}\right), & z < -J\,L \end{cases} \tag{1}$$

Here, $\rho_0 = \rho(0^+)$ represents the characteristic density, located just above the top step. Above and below the staircase, the (constant) squared buoyancy frequency is $N_0^2 \equiv -(g/\rho_0)d\bar{\rho}/dz = g'L$, in which $g' = g\Delta\rho/\rho_0$ is the reduced gravity. This sets the size of the density jumps

$\Delta\rho$ within the staircase for given step depth, L. The density jump at the top and bottom step is $\Delta\rho/2$.

The spatio-temporal structure of disturbances outside and within the staircase are assumed to be horizontally periodic with wavenumber k and (possibly complex) frequency ω. In terms of the streamfunction, the structure is given by $\psi(x,z,t) = \hat{\psi}(z)\exp[\imath(kx-\omega t)]$, in which it is understood that the actual streamfunction is the real part of this expression. The vertical structure of the streamfunction, $\hat{\psi}$, satisfies the following equation (e.g. see Sutherland [2]):

$$\frac{d^2\,\hat{\psi}}{dz^2} + k^2\left(\frac{N^2}{\omega^2}-1\right)\hat{\psi} = 0. \tag{2}$$

Because $N = N_0$ is constant above and below the staircase and $N = 0$ within each step of the staircase, piecewise-analytic general solutions can be found for $\hat{\psi}(z)$ of the form

$$\hat{\psi}(z) = \begin{cases} A_0\,e^{\imath mz} + B_0\,e^{-\imath mz}, \quad \text{for } z>0 \\ A_j\,e^{k[z+L(j-1/2)]} + B_j\,e^{-k[z+L(j-1/2)]}, \quad -jL<z<-(j-1)L, \quad j=1\ldots J \\ A_{J+1}\,e^{\imath m[z+L\,J]} + B_{J+1}\,e^{-\imath m[z+L\,J]}, \quad \text{for } z<-J\,L. \end{cases} \tag{3}$$

Here, $m \equiv k\sqrt{N_0^2/\omega^2-1}$, represents the (positive) vertical wavenumber of waves above and below the staircase if ω is real and less than N_0. We will see that for natural modes of the staircase, m is complex-valued. In this case, we define m so that its real part is positive.

The constants A_j and B_j for $j = 0,\ldots J+1$ can be found by imposing continuity of vertical velocity and pressure. This amounts to requiring that $\hat{\psi}$ and $d\psi/dz = g\frac{\bar{\rho}}{\rho_0}\frac{k^2}{\omega^2}\hat{\psi}$ are continuous (e.g. see Sec 2.6.1 of Sutherland [2]). This gives a pair of interface conditions at $z = jL$, for $j = 0,\ldots,J$, for a total of $2(J+1)$ equations. These are given in Appendix A.

Full solutions depend upon conditions imposed above and below the staircase. Because the sign of the vertical group velocity, c_g, is opposite to the sign of (the real part of) m, the coefficients A_0 and A_{J+1} correspond to the amplitudes of downward propagating waves, whereas B_0 and B_{J+1} correspond to the amplitudes of upward propagating waves. For the tunneling problem with incident waves propagating downward from above, we take $B_{J+1} = 0$. For the problem of modes, we require waves to propagate away from the staircase so that $A_0 = B_{J+1} = 0$.

B. Tunneling of plane waves

The theory for the transmission of incident plane waves across a density staircase was developed by Sutherland [9]. That study included the effects of rotation and allowed for steps having small random variations in the step size. Here we focus on the analytic solutions where the step size, L, is same for all steps, and we ignore background rotation.

Setting $B_{J+1} = 0$ in (3), and applying the interface conditions gives $2J + 2$ equations in $2J + 3$ unknowns. These can be combined to get an explicit expression for A_0 in terms of A_{J+1}:

$$A_0 = \frac{i}{4M}(a_+, a_-)\, \mathcal{C}^{J-1} \begin{pmatrix} a_+ \\ a_- \end{pmatrix} A_{J+1}, \tag{4}$$

in which the left and right vectors have components

$$a_\pm \equiv \Delta^{\pm 1/2}\, [1 \mp \Gamma \pm iM], \tag{5}$$

the matrix $\mathcal{C}$ is

$$\mathcal{C} = \begin{pmatrix} \Delta(1-\Gamma) & -\Gamma \\ \Gamma & \Delta^{-1}(1+\Gamma) \end{pmatrix}, \tag{6}$$

and we have defined the following nondimensional quantities:

$$\Delta \equiv \exp(kL),\ M \equiv m/k = \sqrt{\tfrac{N_0^2}{\omega^2} - 1},\ \Gamma \equiv \tfrac{g' k^2}{2k\ \omega^2} = \tfrac{1}{2}kL(M^2+1). \tag{7}$$

In the expressions for M and Γ we have used the dispersion relation where $N^2 = N_0^2$ is constant: $\omega^2 = N_0^2 k^2/(k^2 + m^2)$.

An analytic solution to (4) is found by diagonalizing $\mathcal{C}$ in terms of its eigenvalues, $\lambda_\pm$. From this solution an expression for the transmission coefficient is found: $T = |A_{J+1}/A_0|^2$, which represents the fraction of the energy (or, equivalently, energy flux) associated with the incident waves that is transmitted below the staircase. Explicitly this is given by [9]

$$T = \frac{1}{1+X^2},\ \text{with } X \equiv \frac{\delta_+\Gamma_+\ +\ \delta_-\Gamma_-\ +\ 2\delta_0\Gamma|\Lambda_-|}{4M|b_0|}, \tag{8}$$

in which

$$\delta_\pm \equiv \Delta^\pm \left[(1 \mp \Gamma)^2 + M^2\right],\ \delta_0 \equiv \Gamma^2 - 1 + M^2, \tag{9}$$

$$\Gamma_\pm = b_-|\Lambda_-|\ \pm\ |b_0|\Lambda_+, \quad \Lambda_\pm = \frac{1}{2}\left[\lambda_+^{J-1} \pm \lambda_-^{J-1}\right], \tag{10}$$

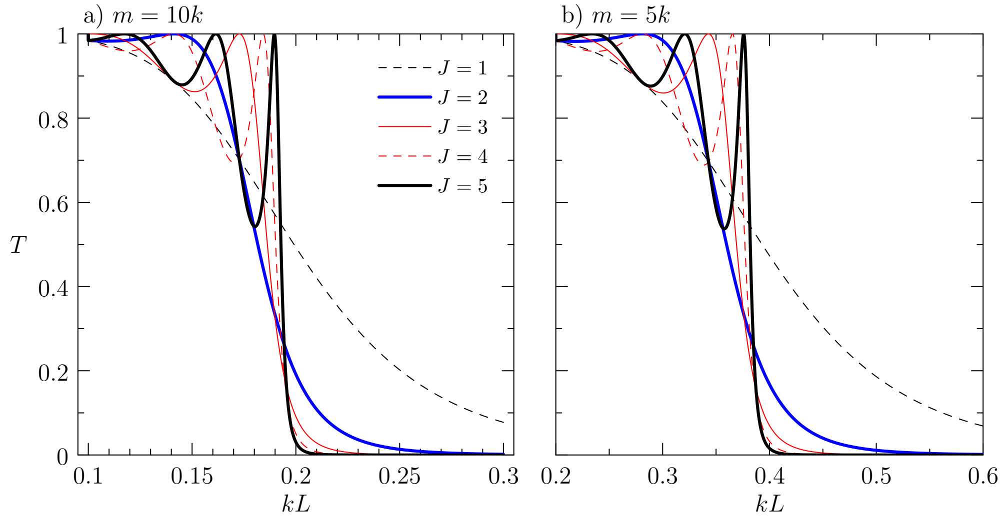

FIG. 1. Predicted transmission coefficient as it depends on the relative step size, kL, and the number of steps, J, for incident plane waves with a) $m = 10k$ ($\omega/N_0 \simeq 0.0995$) and b) $m = 5k$ ($\omega/N_0 \simeq 0.1961$). The different line styles in both plots represent the number of steps, as indicated in a).

$$\lambda_\pm = b_+ \pm b_0, \quad b_\pm \equiv \frac{1}{2}\left[\Delta\left(1-\Gamma\right) \pm \Delta^{-1}\left(1+\Gamma\right)\right], \quad b_0 \equiv \sqrt{b_+^2 - 1}. \tag{11}$$

Examination of T shows that the transition between strong and weak transmission occurs for [9]

$$\omega_c/N_0 = \left[(kL/2)\tanh(kL/2)\right]^{1/2} \simeq kL/2, \tag{12}$$

in which the last expression gives the approximation for $kL \ll 1$. Alternately, given a forcing frequency $\omega_0 \ll N_0$, the critical transition occurs for relative horizontal wavenumber

$$k_c L = 2\omega_0/N_0. \tag{13}$$

Mathematically, the transition corresponds to the condition, $b_0 = 0$, delineating the boundary between real and complex values of $\lambda_\pm$. For frequencies lower than ω_c ($\lambda_\pm$ complex), a series of transmission spikes occurs where $T = 1$. If the staircase has J steps, there are J transmission spikes. This is shown, for example in Figure 1.

In astrophysics, the transmission spikes are said to correspond to "global (g-)modes" [11, 22]. The dispersion relation of these modes can be found by setting $X = 0$ in (8), which is equivalent to setting $B_0 = 0$ (and hence $|A_{J+1}| = A_0$) in (3) and applying the interface conditions to get an eigenvalue problem. In the expression for X, it is readily shown that

$|\Lambda_-|/|b_0|$ and Λ_+ are polynomials in b_0^2. Hence $4MX$ can be written as a polynomial in M^2, whose roots can be found numerically for given kL (e.g. with MATLAB's "vpasolve" function). The corresponding frequency is then found from $\omega/N_0 = (1+M^2)^{-1/2}$.

The resulting dispersion relations for the global modes are plotted in Figures 2a,c) for cases with $J = 2$ and 5 steps. The lowest mode has ω/N_0 nearly constant with kL for small kL. This mode arises from the interfaces at $z = 0$ and $-JL$. For $J > 1$, higher modes exhibit a near-linear dependence upon kL for small kL, with the highest mode having frequency moderately larger than the critical frequency ω_c, given by (12).

C. Interfacial waves resonant modes trapped in a J-steps staircase

Next we find the dispersion relation corresponding to the natural modes of a density staircase. This is found by setting $A_0 = B_{J+1} = 0$ in (3) and applying the interface conditions to get an eigenvalue problem. The resulting eigenvalue problem can be written as a pair of equations for B_0 and A_{J+1}:

$$\begin{pmatrix} a_- \\ a_+ \end{pmatrix} B_0 = \mathcal{C}^{J-1} \begin{pmatrix} a_+ \\ a_- \end{pmatrix} A_{J+1}, \tag{14}$$

in which $a_\pm$ is given by (5) and the matrix $\mathcal{C}$ is given by (6). Casting this as a matrix eigenvalue problem for the eigenvector $(B_0, A_{J+1})^T$, and setting the matrix determinant to zero gives

$$\left[-2\Gamma a_+ a_- + b_-(a_+^2 + a_-^2)\right](\Lambda_0/b_0) + (a_+^2 - a_-^2)\,\Lambda_+ = 0. \tag{15}$$

with Γ, $\Lambda_\pm$, b_- and b_0 defined by (7), (10) and (11).

As with the problem of finding global modes, Λ_+ and Λ_-/b_0 are expressions involving b_0^2. Hence (15) reduces to the problem of finding the roots of a polynomial in M^2. Unlike the global modes, the eigenvalues, $m = Mk$, are complex, as are the corresponding frequencies $\omega = N_0/(1+M^2)^{1/2}$. This result can be contrasted with the study of Belyaev et al [22] who found only real-valued frequencies in their dispersion relation for modes in an effectively infinite staircase (with periodic upper and lower boundary conditions). Taking eigenvalues with the real part of M to be positive, we find the complex frequencies have positive real parts, ω_r, and negative imaginary parts, ω_i. Hence the modes decay exponentially in time with an

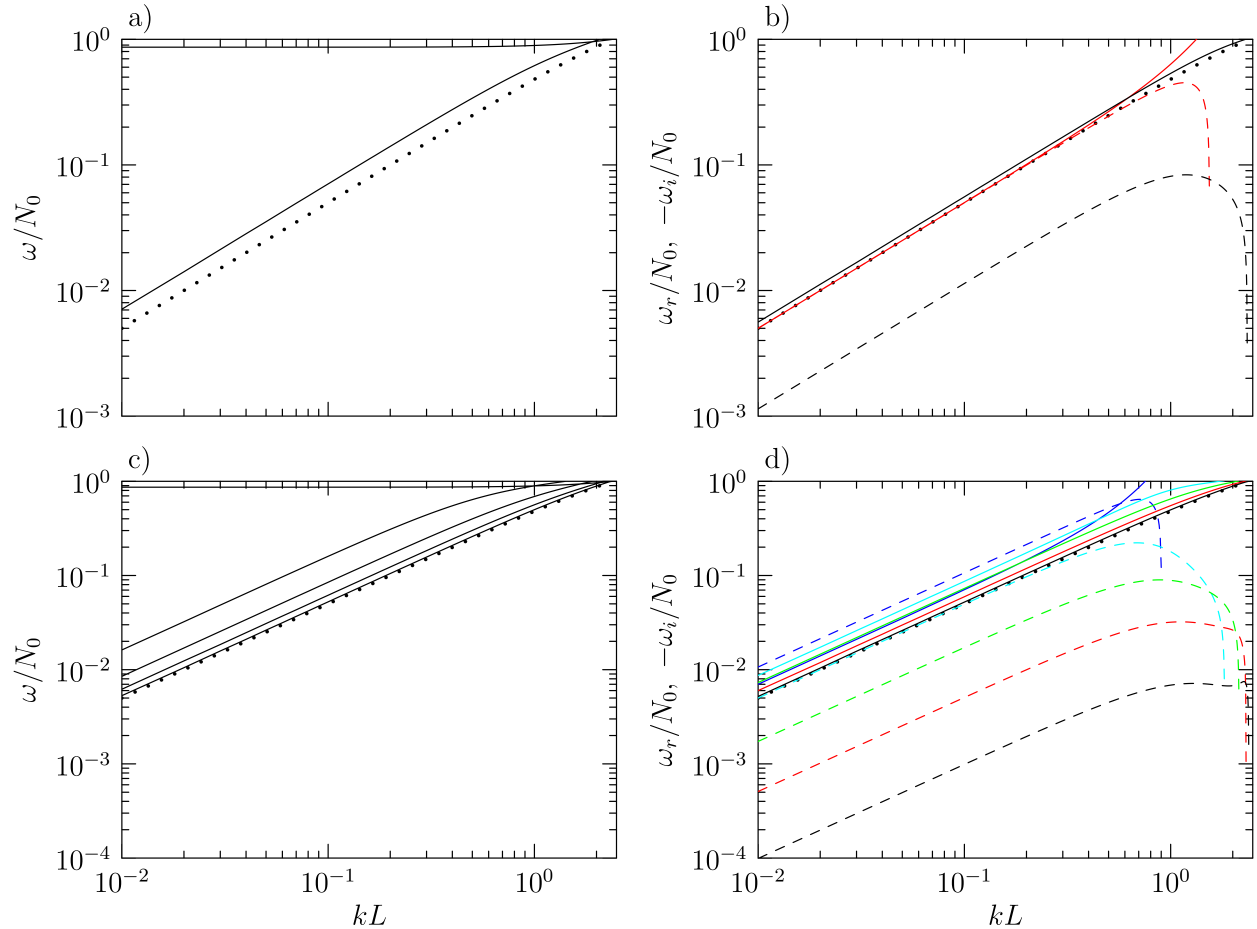

FIG. 2. Log-log plots of the dispersion relation for a,c) global modes and b,d) natural modes of a density staircase having a,b) $J = 2$ steps and c,d) $J = 5$ steps. In all four plots, the dotted black line is the critical frequency ω_c, given by (12). In b,d) the solid and dashed lines correspond, respectively, to the real and (negative) imaginary part of the frequency. The colours indicate the mode number with the highest vertical mode (lowest frequency at fixed kL) drawn as solid and dashed black lines.

e-folding time $1/|\omega_i|$, as is expected for modes that continuously lose energy to upward and downward propagating internal waves, respectively above and below the staircase.

The dispersion relations of modes in staircases with $J = 2$ and $J = 5$ are plotted in Fig. 2b,d). Like the global modes, the largest vertical mode (with lowest frequency at fixed kL) has frequency moderately larger than the critical frequency, ω_c, and also has the lowest magnitude of the decay rate, $|\omega_i|$.

The overlap between the dispersion relation of global modes and the real part of the dispersion relation of the natural modes with large vertical mode number was anticipated, with higher transmission expected when incident plane waves are near-resonant with natural modes of the system. However, the resonance is never exact because the natural modes are not steady, but decay in time. Furthermore, the imaginary part of the eigenvalues of $M = (m_r + im_i)/k$ for the modes are negative. Thus, while the vertical structure of the modes oscillate above and below the staircase with vertical wavenumber m_r, they also grow exponentially with e-folding scale $1/|m_i|$. This is a result of the normal mode solutions representing an effectively infinitely large disturbance in the staircase as $t \to -\infty$ that propagates vertically away from the staircase at the group velocity as the disturbance in the staircase decays exponentially in time.

We are particularly interested in the dependence upon the number of steps, J, of the decay rate of the highest vertical mode. An approximate analytic expression can be found in the limit $kL \ll 1$ and $J \gg 1$. Because the highest vertical mode is near the critical transition, $\omega_c/N_0 \simeq kL/2$, we require $\omega/N_0 \ll 1$. Hence, using $\omega/N_0 = (M^2+1)^{-1/2}$, we must have $|M| \gg 1$ and $\omega/N_0 \simeq 1/M = k/m$. Explicitly, we suppose the relative vertical wavenumber of the highest mode can be written as $\tilde{m} \equiv mL = 2 - \epsilon$, in which ϵ is complex-valued and $|\epsilon| \ll 1$. The perturbation calculation, described in Appendix B, gives $\epsilon \simeq (3/2)J^{-2} - 3iJ^{-3}$. From this it follows that the approximate dispersion relation of the highest vertical mode is

$$\frac{\omega}{N_0} \simeq \frac{kL}{2}\Big(1 + \frac{3}{4}J^{-2} - \frac{3}{2}i\, J^{-3}\Big). \tag{16}$$

In particular, this shows that the decay rate of the mode decreases with the number of steps as J^{-3}. The predicted e-folding time scale, τ_e, associated with the decay of energy is given by

$$N_0\tau_e = \frac{2}{3}\frac{1}{kL}J^3 \tag{17}$$

D. Resonant mode excitation

The unbounded spatial growth of modes above and below the wavepacket is an artifact of seeking normal mode solutions. In reality, the modes are excited transiently by the incident wavepacket, and so the vertical extent of the mode structure is limited by the time over which the mode is excited. This provides a theoretical challenge in predicting the maximum amplitude to which modes are excited by the incident wavepacket. Specifically, even though the partial differential equation which gives the dispersion relation and vertical structure of the modes is of Sturm-Liouville form, this is not a Sturm-Liouville problem in that the domain is vertically unbounded and the modes themselves are unbounded as $|z| \to \infty$. Hence there is no orthogonality relationship between different modes.

Here we proceed to develop an approximate theory for the excitation of modes by an incident wavepacket with the intent to demonstrate that significant excitation occurs only if the incident wave frequency is near-resonant with the (real) frequency of the mode and if mode decays slowly in time compared with the transient time over which the mode is forced by the incident waves. These two conditions are met only if the incident wave is near-resonant with the highest frequency mode near the critical transition between high and low transmission.

For small amplitude incident waves and modes, the equation for the excitation of modes can be written in terms of the streamfunction:

$$\sum_j [\partial_{tt}\nabla^2 + N^2\partial_{xx}]\psi_j = -[\partial_{tt}\nabla^2 + N^2\partial_{xx}]\psi_I, \tag{18}$$

in which (the real part of) $\psi_j = a_j(t)\hat{\psi}_j(z)\exp[i(kx - \omega_j t)]$ describes the streamfunction of mode-j whose amplitude $a_j(t)$ denotes the evolution of its magnitude in response to the forcing. We model the interaction of the wavepacket with the staircase as a forcing within the staircase whose amplitude grows and decays in time as $a_0(t)$, so that the corresponding streamfunction is (the real part of) $\psi_I = a_0(t)\hat{\psi}_I(z)\exp[i(kx - \omega_0 t)]$. For the incident Gaussian wavepacket of our numerical study (see Sec. III), the forcing amplitude is given explicitly by

$$a_0(t) = A_0 \exp[-t^2/(2\tau_0^2)]. \tag{19}$$

Here, $\tau_0 = \sigma_0/c_g$, in which σ_0 is the spatial extent of the incident wavepacket and c_g is the magnitude of its vertical group velocity. As such, τ_0 is the time scale for growth and decay of the forcing. Here we have defined time so that a_0 is largest at $t = 0$.

We assume the time-scales for the evolution of a_0 and a_j are long compared to the time-scales, $1/\omega_0$ and $1/|\omega_j|$, of the incident waves and modes, respectively, in which $|\omega_j|$ is the magnitude of the complex-valued frequency ω_j. Hence, from (18), the leading-order time-evolution equation for a_j and a_0 is

$$\sum_j \dot{a}_j \ (N^2/\omega_j)\hat{\psi}_j \exp[i(kx - \omega_j t)] = -\dot{a}_0 \ (N^2/\omega_0)\hat{\psi}_0 \exp[i(kx - \omega_0 t)], \tag{20}$$

in which the dots on a_j and a_0 denote time derivatives. In deriving (20) we have we have used the dispersion relation for the modes and the incident wave (assuming ω_0 is constant) as well as the vertical structure equation (2).

In previous studies examining forcing of mean flows by vertically bounded internal modes, equations for the evolution of each vertical mode could be found using orthogonality of the vertical modes with respect to the weight N^2 [23]. This methodology cannot be applied to extract explicit equations for a_j from the sum in (20) because the modes are not orthogonal. We expect modes will be excited to non-negligible amplitudes only if the real part of ω_j is comparable to ω_0, thus resulting in near-resonant excitation. This leads us to estimate an approximate evolution for the amplitude of a near-resonant mode with mode-number j:

$$\dot{a}_j \simeq -C_j \ \frac{\omega_j}{\omega_0} \dot{a}_0 \exp[-i(\omega_I - \omega_j)t]. \tag{21}$$

Here we have defined the interaction coefficient, C_j, assuming that the vertical forcing of the mode is driven primarily by motion within the staircase:

$$C_j = \big[\int_{-JL^-}^{0^+} \Re\{\hat{\psi}_j^\star \hat{\psi}_0\} N^2 \, dz\big] / \big[\int_{-JL^-}^{0^+} |\hat{\psi}_j|^2 N^2 \, dz\big], \tag{22}$$

in which $\Re$ denotes taking the real part. The bounds on the integrals are set to include the density jumps at the top and bottom of the staircase. In evaluating the integrals, N^2 can be treated as proportional to a Dirac delta function, $\delta(z)$, with proportionality constant given by the density jump. Explicitly, $N^2(0) = (g'/2)\,\delta(0) = (N_0^2 L/2)\,\delta(0)$, $N^2(-JL) = (N_0^2 L/2)\,\delta(z + JL)$, and $N^2(-jL) = N_0^2 L\,\delta(z + jL)$ for $j = 1, \ldots J-1$. Thus C_j can be expressed explicitly in terms of the known coefficients, A_j and B_j of the vertical structure functions of the mode and tunnelling waves (see Appendix A).

To solve (21), we specify an initial condition on the amplitude of the mode at a finite, but large (negative) time: $a_j(-t_0) = 0$ for some $t_0 \gg \tau_0$. Using (19) in (21), and integrating both sides in time from $-t_0$ to some time t gives

$$\begin{aligned} a_j(t) = -C_j \tfrac{\omega_j}{\omega_0} a_0 \Big[\ & e^{-t^2/(2\tau_0^2)} e^{\Sigma t} - e^{-t_0^2/(2\tau_0^2)} e^{-\Sigma t_0} \\ & -\sqrt{\tfrac{\pi}{2}}\, \Sigma\tau_0\, e^{(\Sigma\tau_0)^2/2} \left(\mathrm{erf}\big[\tfrac{1}{\sqrt{2}}(\tfrac{t}{\tau_0} - \Sigma\tau_0)\big] - \mathrm{erf}\big[\tfrac{1}{\sqrt{2}}(\tfrac{t_0}{\tau_0} - \Sigma\tau_0)\big] \right) \Big]. \end{aligned} \tag{23}$$

Here we have defined $\Sigma = 1/\tau_j - i\Delta\omega$, in which $\tau_j = -1/\omega_{ji}$ is the (positive) e-folding decay time associated with the imaginary part of the frequency of mode-j, ω_{ji}, and $\Delta\omega \equiv \omega_0 - \omega_{jr}$ is the difference of the forcing frequency and the real part of the frequency of mode-j, ω_{jr}.

The error function in (23) has a complex argument, which can be written explicitly in terms of its real and imaginary parts using

$$\operatorname{erf}(a+ib) = \operatorname{erf}(a) + i\frac{2}{\sqrt{\pi}} e^{-a^2} \int_0^b e^{2ias} e^{s^2}\, ds. \tag{24}$$

In particular, the second term can be neglected if $|a| \gg |b|$.

We seek the amplitude of the mode when the forcing reaches its peak at $t = 0$. Assuming $t_0 \gg \tau_0$, we find

$$\begin{aligned} a_j(0) = -C_j \tfrac{\omega_j}{\omega_0} a_0 \Big[\; & 1 - \sqrt{\tfrac{\pi}{2}}\, \Sigma\tau_0 \, e^{(\Sigma\tau_0)^2/2} \operatorname{erfc}\big(\tfrac{\tau_0}{\sqrt{2}\tau_j}\big) \\ & + i\sqrt{2}\Sigma\tau_0 \, e^{-i\Delta\omega\tau_0^2/\tau_j} e^{-(\Delta\omega\tau_0)^2/2} \textstyle\int_0^{\Delta\omega\tau_0/\sqrt{2}} e^{i\sqrt{2}\tau_0 s/\tau_j}\, e^{s^2}\, ds \Big]. \end{aligned} \tag{25}$$

Although this can be evaluated numerically, it is useful to consider two limits.

If $\tau_j \ll \tau_0$, the asymptotic approximation to erfc and the integral in (25) give the leading order expression

$$a_j(0) \simeq a_0 C_j \frac{\omega_j}{\omega_0} \left[\big(\frac{\tau_j}{\tau_0}\big)^2 - 2(1 - i\Delta\omega\, \tau_j)\Big(1 - e^{-(\Delta\omega\tau_0)^2/2} e^{-i\Delta\omega\, \tau_0^2/\tau_j}\Big) \right], \quad \tau_j \ll \tau_0. \tag{26}$$

Thus, even if the frequency of the incident wave is nearly resonant with the (real) frequency of the mode, the mode is not excited to large amplitude.

If $\tau_j \gg \tau_0$, (25) is given approximately by

$$a_j(0) \simeq a_0 C_j \frac{\omega_j}{\omega_0} \begin{cases} -i\sqrt{\frac{\pi}{2}} \Delta\omega\tau_0 e^{-(\Delta\omega\tau_0)^2/2}, & |\Delta\omega\, \tau_0/\sqrt{2}| \gg 1, \\ \;\; 1 - \sqrt{\frac{\pi}{2}}\big(\frac{\tau_0}{\tau_j} - i\Delta\omega\tau_0\big), & |\Delta\omega\, \tau_0/\sqrt{2}| \ll 1. \end{cases} \tag{27}$$

Thus, even if the mode decays slowly, it is not excited to large amplitude if the incident wave is not resonant with the mode. Only if the incident wave is nearly resonant with a slowly decaying mode is it excited to significant amplitude. This would be the case if the incident wave frequency is close to the highest frequency mode near a transmission spike.

Given the amplitudes, $a_j(0)$, we go on to estimate the "initial" energy of the excited mode:

$$E_j(0) = \frac{1}{2}|a_j(0)|^2 \frac{k^2}{|\omega_j|^2} \int_{-JL^-}^{0^+} N^2 |\hat{\psi}_j|^2 dz. \tag{28}$$

As the forcing from the incident wave decreases for $t \gg \tau_0$, the energy of the mode is expected to decay as $E_j(t) \sim E_j(0) \exp(-2t/\tau_j)$.

III. NUMERICAL SIMULATIONS

We use a numerical code that solves the fully nonlinear two-dimensional, Boussinesq equations cast in terms of the spanwise vorticity, $\zeta \equiv \partial_z u - \partial_x w$, and buoyancy, b:

$$\frac{D\zeta}{Dt} = -\frac{\partial b}{\partial x} + \nu \mathcal{D}_\zeta, \qquad \frac{Db}{Dt} = -N^2 w + \kappa \mathcal{D}_b, \tag{29}$$

in which $D/D_t = \partial_t + \vec{u}\cdot\nabla$ is the material derivative, $\vec{u} = (u, w)$ is the velocity with horizontal (x) and vertical (z) components u and w, respectively, and $\nabla = (\partial_x, \partial_z)$. The fields are discretized vertically on an evenly spaced grid and are represented horizontally in Fourier space. The effect of viscosity and diffusion is represented by the operator $\mathcal{D}$. This is the Laplacian operator in horizontal Fourier space, $-k_n^2 + \partial_{zz}$, except that it operates only upon horizontal wavenumbers, k_n, above a specified cut-off taken to be $k_\star = 32k$. In this way diffusion acts to damp small-scale numerical noise, but does not act upon the waves associated with the wavepacket, having horizontal wavenumber k, and the modes it excites. The viscous and diffusion coefficients are taken to be $\nu = \kappa = 100000 N_0 k^{-2}$. At each time step, the streamfunction is found through inversion of the Laplacian equation $\nabla^2\psi = -\zeta$. From this the velocity components are found by $u = -\partial_z\psi$ and $w = \partial_x\psi$.

In the idealized staircase used by our theory, the density jumps discontinuously at each step. So that N^2 is finite, but still representative of rapid density jumps, we define a background density profile, $\rho\bar{(z)}$, similar to (1) but with continuously varying density that increases with depth across each step over a thickness scale, typically taken to be $\sigma_N = 0.01L$. For a staircase with J steps, the density profile is given explicitly by

$$\begin{aligned}
\bar{\rho}(z) \;=\; & \rho_0 - \frac{1}{2}\rho_0\frac{N_0^2}{g}[z + \sigma_N \ln\cosh(z/\sigma_N)] + \frac{1}{2}\Delta\rho[1 - \tanh(z/\sigma_N)] \\
& + \sum_{j=1}^{J-1}\Delta\rho[1 - \tanh((z + jL)/\sigma_N)] \\
& + \frac{1}{2}\rho_0\frac{N_0^2}{g}\Big[- z + \sigma_N \ln\left(\frac{\cosh((z+JL)/\sigma_N)}{\cosh(JL/\sigma_N)}\right)\Big] \\
& + \frac{1}{2}\Delta\rho\Big[1 - \tanh\left(\frac{z+JL}{\sigma_N}\right)\Big].
\end{aligned} \tag{30}$$

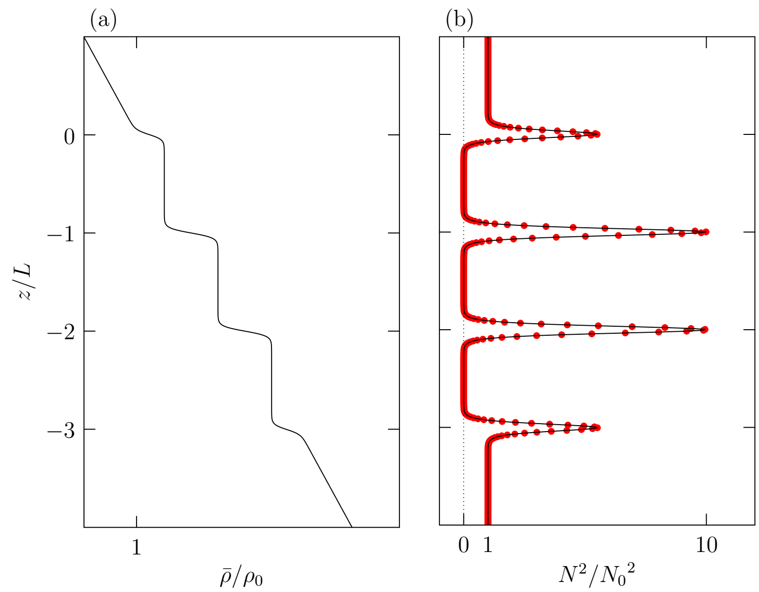

FIG. 3. Profiles used in numerical simulations of a) background density $\bar{\rho}(z)$ and b) background stratification $N^2(z)$, for $J = 3$. The red dots in b) indicate the vertical resolution of the numerical model.

Using $g' = g\Delta\rho/\rho_0 = N_0^2 L$, the corresponding N^2 profile is given by

$$\begin{aligned} N^2(z)/N_0^2 \;=\;& \frac{1}{2}\Big[1 + \tanh(z/\sigma_N) + \frac{1}{2}\frac{L}{\sigma_N}\,\mathrm{sech}^2(z/\sigma_N)\Big] \\ &+ \sum_{j=1}^{J-1} \frac{1}{2}\frac{L}{\sigma_N}\,\mathrm{sech}^2\big((z + jL)/\sigma_N\big) \\ &+ \frac{1}{2}\Big[1 - \tanh\big((z + JL)/\sigma_N\big) + \frac{1}{2}\frac{L}{\sigma_N}\,\mathrm{sech}^2\big((z + jL)/\sigma_N\big)\Big] \end{aligned} \tag{31}$$

These profiles are plotted for the case $J = 3$ in Fig 3.

Superimposed on the background stratification, the simulations were initialized with a horizontally periodic, vertically compact quasi-monochromatic wavepacket having a Gaussian amplitude envelope centered at $z = z_0$. In terms of the streamfunction the wavepacket is defined by,

$$\psi(x, z, t = 0) = \mathcal{A}_{\psi 0}\, \exp\left[-\frac{1}{2}\left(\frac{z - z_0}{\sigma_0}\right)^2\right] \cos(kx + m_0 z) \tag{32}$$

in which k and m_0 respectively, are the horizontal and peak vertical wavenumbers, $\mathcal{A}_{\psi 0}$ is the maximum streamfunction amplitude, and σ_0 is the vertical extent of the wavepacket. In all simulations we set $\sigma_0 m_0 = 10$, so that the wavepacket is quasi-monochromatic with peak frequency $\omega_0 = N_0 k/(k^2 + m_0^2)^{1/2}$. The initial wavepacket is centered at $z_0 = 10k^{-1} \gg \sigma_0$ so that the wavepacket has negligible amplitude within the staircase at the start of the simulation. From the polarization relations for monochromatic waves, the initial spanwise vorticity and buoyancy are specified in terms of the streamfunction by $\zeta|_{t=0} = (k^2{+}m_0^2)\,\psi|_{t=0}$ and $b|_{t=0} = N_0^2(k/\omega_0)\,\psi|_{t=0}$,

In our simulations there was no mean background flow. Nevertheless, we computed the Eulerian-induced mean flow, u_E, generated by the wavepacket and superimposed this on the background. Explicitly, the wave-induced mean flow is defined in terms of ζ and b by $u_E(z, t = 0) = \langle \zeta\; b\rangle / N_0^2$ (e.g. see Sutherland [2]). The presence of the induced flow is included by adding $-du_E/dz$ to the background vorticity field.

The simulations were performed in a horizontally periodic domain with one horizontal wavelength of the incident wavepacket spanning the horizontal extent. The vertical extent needed to be sufficiently tall for the disturbance in the staircase to reach negligibly small amplitude before the transmitted and reflected waves reached the top and bottom of the domain, respectively. Thus we set $-H \leq z \leq H$, with $H = 60L$. In order to resolve the spikes in N^2, high vertical resolution was required with typical simulations having 2^16 points in the vertical, giving a vertical resolution of $\Delta z \simeq 0.0018L$. This resolution is indicated by the red dots in Fig. 3b. The horizontal field was represented by a superposition of 64 Fourier modes. Simulations were advanced in time using a leapfrog scheme for advective terms, with an Euler backstep taken every 20 steps. Each time step had a resolution of $\Delta t = 0.05N_0^{-1}$.

In all simulations the time scale was set so that $N_0 = 1$ and the length scale was set so that $k = 1$. Nonetheless, the results are presented with these scales being explicitly represented. We conducted a range of simulations with the number of steps in the staircase ranging from $J = 1$ to 10. The relative vertical wavenumber of the incident wavepacket, m_0/k, was 5 or 10, corresponding to $\omega_0/N_0 \simeq 0.2$ or 0.1, respectively. According to (12), the predicted transition between weak and strong transmission with $kL \ll 1$ occurs for $\omega_c \simeq kL/2$. To explore this transition, in simulations with $m_0/k = 5$, kL ranged from 0.2 to 0.55; in simulations with $m_0/k = 10$, kL ranged from 0.1 to 0.3.

We also conducted a range of simulations varying the initial wavepacket amplitude. In terms of the initial vertical displacement amplitude, $\mathcal{A}_0 = (k/\omega)\,\mathcal{A}_{\psi 0}$, our simulations had amplitudes with $\mathcal{A}_0 k$ ranging from 0.001 to 0.01. In this range there was no significant quantitative difference between simulation results in terms of transmission and reflection diagnostics. Hence, we report here only upon simulations with $\mathcal{A}_0 k = 0.001$. The sensitivity of results to the interface thickness was examined by performing some simulations with half the interface thickness ($\sigma_N = 0.005L$) and double the vertical resolution. No significant quantitative differences to our results were found.

The analysis of our simulations focused upon the evolution of energy over time above, within, and below the staircase. At each time, we calculated the total horizontally averaged, vertically integrated energy, E_{total}. This was partitioned into the energy above, within and below the staircase respectively by the integrals

$$E_r = \int_{z=3\sigma_N}^{H} (\text{KE} + \text{PE})\, dz \tag{33}$$

$$E_s = \int_{z=-JL-3\sigma_N}^{3\sigma_N} (\text{KE} + \text{PE})\, dz, \tag{34}$$

$$E_t = \int_{z=-H}^{-JL-3\sigma_N} (\text{KE} + \text{PE})\, dz \tag{35}$$

in which $\text{KE}(z,t) = (1/2)\left\langle u^2 + w^2 \right\rangle$ is the horizontally averaged kinetic energy per mass and $\text{PE}(z,t) = (1/2)\left\langle b^2 \right\rangle / N^2$ is the horizontally averaged available potential energy. Within the staircase $||b|| \to 0$ as $N \to 0$ such that $\text{PE} \to 0$. Hence, in calculating the integral of PE in (34), we do so only where N^2 exceeds a threshold of 0.001.

From the energy integrals, we compute the time-evolving transmission coefficient ($T(t)$) and reflection coefficient ($R(t)$) as well as the relative energy in the staircase ($S(t)$):

$$T(t) = \frac{E_t}{E_{\text{total}}}, \quad R(t) = \frac{E_r}{E_{\text{total}}}, \quad S(t) = \frac{E_s}{E_{\text{total}}}. \tag{36}$$

The duration of the simulations varied primarily based on the vertical group velocity of the incident wavepacket and the number of steps, J, in the staircase. As we show, for larger J, energy remains trapped in the staircase for longer times, requiring longer simulations. In most simulations, the final time was set so that the relative energy within the staircase, $S(t)$, fell below 0.001 after reaching its peak. In the simulation with $J = 10$, the waves reached the top and bottom of the domain before this threshold was reached. These simulations were terminated at time $6590 N_0^{-1}$ when $S(t) \simeq 0.0065$.

We will show that energy persists for longer times in a staircase with a larger number of steps due to the excitation of modes with long e-folding decay times. To quantify this, we constructed a log-plot of the energy within staircase, $\ln(S(t))$ versus t, and found the slope of the best-fit line through over late times for which $S \leq 0.01$. The slope determined the e-folding energy decay time, τ_e, within the staircase, which could be compared with the predicted decay time, $2/\tau_j$, of each mode.

IV. RESULTS

We begin with a qualitative examination of wavepacket tunnelling in a simulation of an initial wavepacket having $m_0 = 10k$ being incident upon a staircase with $J = 5$ steps. The peak frequency of the incident wave is $\omega_0 \simeq 0.0995$. We examine the case with $kL = 0.2$, which corresponds to waves near the transition between weak and strong transmission, given by (13). This wavenumber is moderately larger than the predicted largest relative wavenumber of the transmission spikes, which occurs at $kL \simeq 0.19$ (see Fig. 1a). We note that, for $kL = 0.2$, the predicted transmission coefficient is $\simeq 0.5$ for $J = 1$, but is predicted to be small for $J = 5$.

Snapshots of the wavepacket evolution at three times are shown in Fig. 4. The structure of the waves is represented here in terms of the horizontal velocity field normalized by the initial amplitude, $\mathcal{A}_{u0} = m_0 \mathcal{A}_{\psi 0}$. Initially the wavepacket is centered at $z_0 = 10k^{-1}$. The width of the envelope, $10/m_0 = k^{-1}$, is much smaller than z_0 so that the signal of the initial wavepacket within that staircase is negligible.

The vertical group velocity of the wavepacket is $\simeq -N_0 k/m_0^2$. And so the estimated time for the center of the wavepacket to reach the top of the staircase (at $z = 0$) is $z_0 m_0^2/(kN_0) = 1000/N_0$. This is the time shown in Fig. 4b. At this time, the leading flank of the incident wavepacket has partially transmitted through the staircase, as evident from the pattern of downward propagating waves below $z = -JL = -k^{-1}$. Above the top of the staircase the disturbance field is a superposition of the incident trailing flank of the wavepacket and partially reflected upward propagating waves.

At $N_0 t = 2000$ (Fig. 4c), the transmitted waves below the staircase and the reflected waves above the staircase are broadly distributed in the vertical, but disturbances within the staircase are non-negligible. This simulation thus gives qualitative evidence for the excitation of natural modes of the staircase by the traversing incident wavepacket.

To illustrate the impact of the incident wave upon disturbances within the staircase, Fig. 5a shows a close-up view of the staircase region at time $N_0 t = 2000$, corresponding

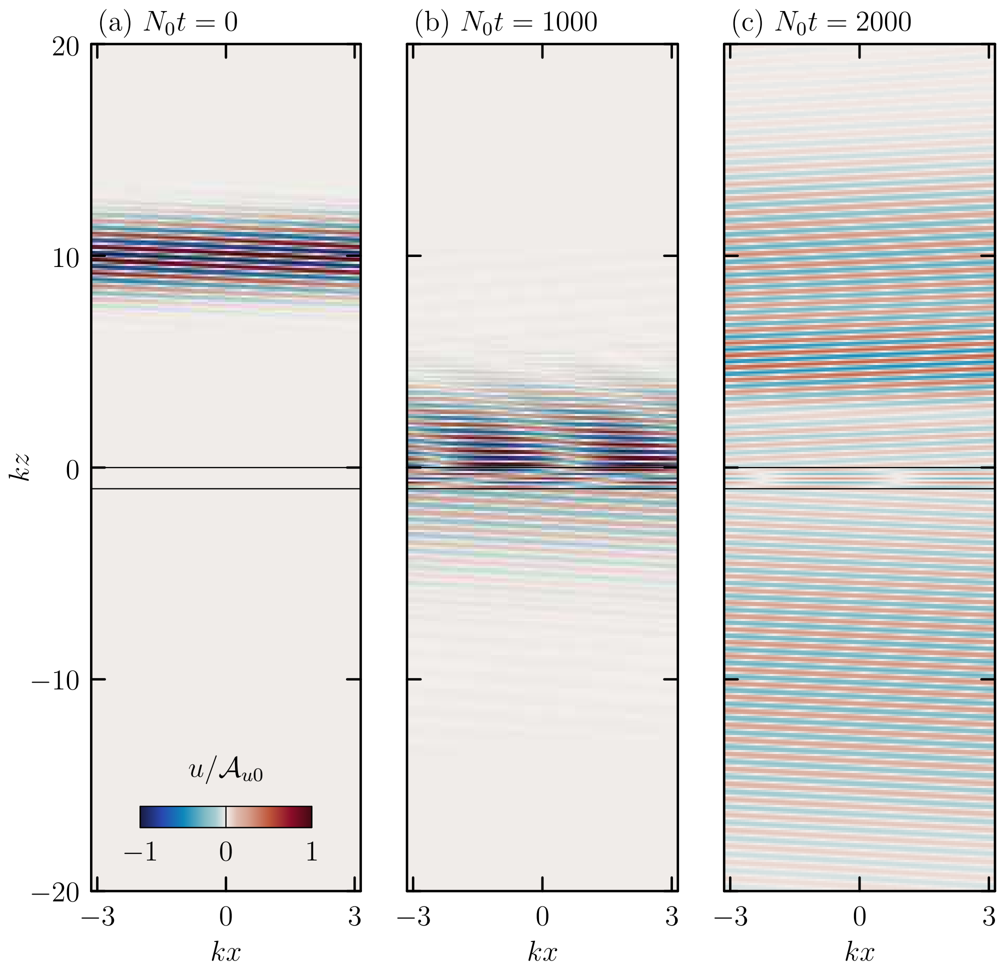

FIG. 4. From a simulation with $m_0 = 10k$, $kL = 0.2$ and $J = 5$, snapshots of horizontal velocity at times a) $t = 0$, b) $1000N_0^{-1}$ and c) $2000N_0^{-1}$. The colours in all three plots show the horizontal velocity normalized by the initial horizontal velocity amplitude $\mathcal{A}_{u0}$, with values indicated by the scale in a). The horizontal lines at $z = 0$ and $z = -1$ indicate the levels at the top and bottom of the staircase, respectively.

to Fig. 4c. Near-monochromatic waves are evident above and below the staircase by phase lines having approximately constant slope. In contrast, disturbances within the staircase have a standing wave pattern, evident both in the horizontal velocity field and isopycnal displacements. The latter are found in terms of the buoyancy field at the center of each interface by computing $\xi = -b/N^2$. The isopycnal displacements exhibit an alternating varicose pattern associated with bulging and pinching contours. As our energy analysis below demonstrates, the disturbances within and near the staircase correspond to a trapped mode that emits internal waves above and below the staircase as the amplitude of disturbances

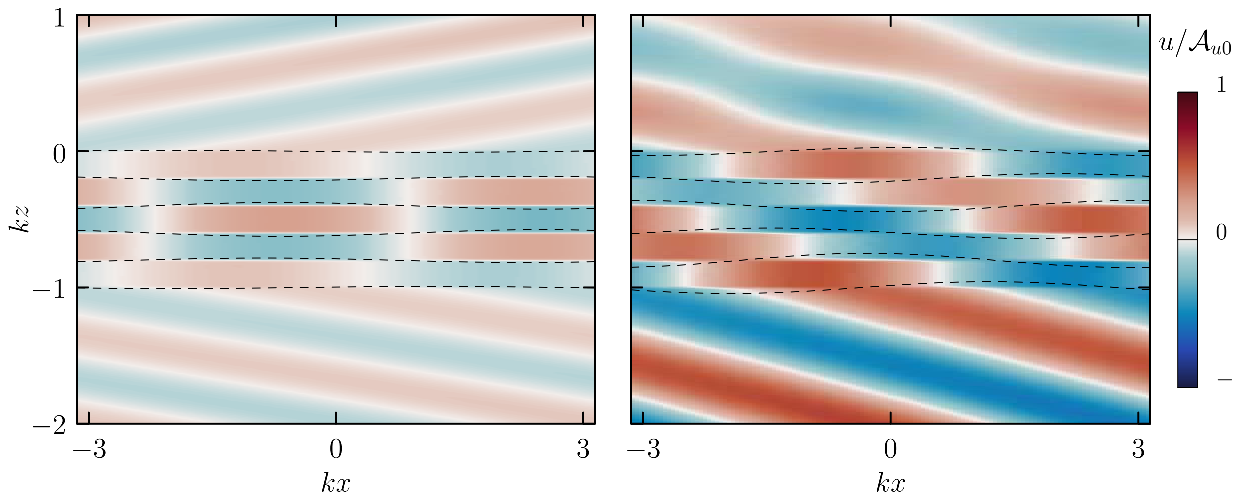

FIG. 5. Horizontal velocity field and isopycnal displacements at each density interface in simulations with $J = 5$, $kL = 0.2$ and a) $m_0 = 10k$ at time $t = 2000\, N_0^{-1}$ and b) $m_0 = 5k$ at time $t = 500\, N_0^{-1}$. The plot in a) corresponds to the snapshot shown in in Fig. 4c, but focused on the vertical region about the staircase.situated between $-1 \leq kz \leq 0$. The dashed lines show the vertical displacement of isopycnals at the center of each interface (at $z = -jL = -0.2j\, k^{-1}$, $j = 0 \ldots 5$). For clarity, the displacements have been magnified by a factor of 100 in a) and by a factor 20 in b).

with the staircase decay exponentially in time.

By contrast, in Fig. 5b we show a snapshot of the horizontal velocity field and isopycnal displacements from a simulation with $J = 5$ and $kL = 0.2$ but with $m_0 = 5k$. Because the vertical group velocity of the incident wavepacket is approximately 4 times larger than the wavepacket with $m_0 = 10k$, we show the snapshot at time $500N_0^{-1}$, which is one quarter of the time of the snapshot shown in Fig. 5a. For this simulation, tunnelling theory for plane waves predicts near-perfect transmission of the wavepacket across the staircase. This is evident in the simulation which shows downward-sloping phase lines above and below the staircase, corresponding to downward propagating waves. Although the phase lines are vertical within each step, the phase shift across each interface corresponds to the expected change for waves unimpeded by the staircase. In a simulation with $m_0 = 5k$ but $kL = 0.4$, which is close to the transition wavenumber, we once again observe the standing wave pattern of horizontal velocity and isopycnal displacements as in Fig. 5a (not shown).

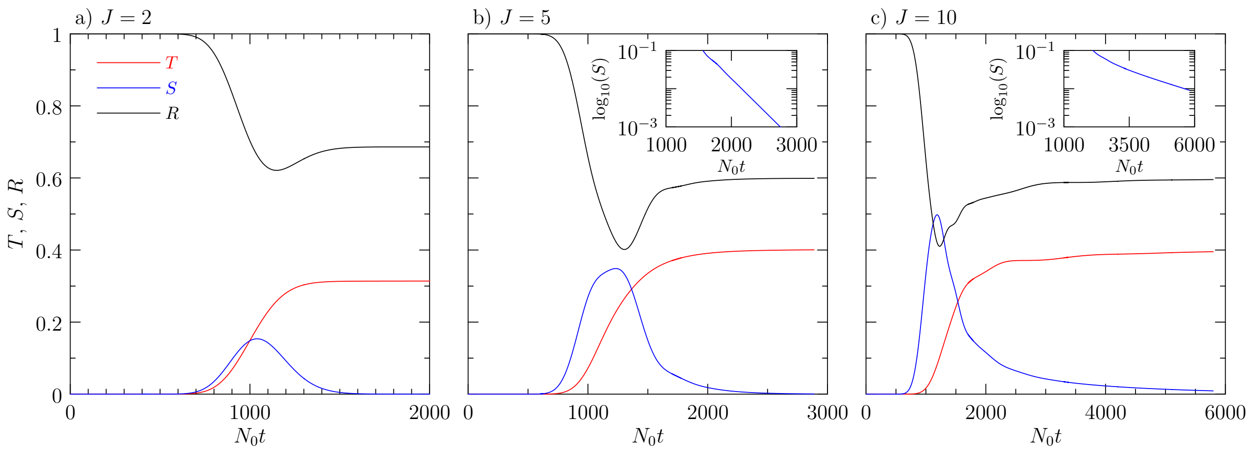

FIG. 6. Time series of the evolution of transmitted energy, T (red line), reflected energy, R (black line), and energy within the staircase, $S(t)$ (blue line) in simulations with a) $J = 2$, b) $J = 5$ and c) $J = 10$ steps. The insets in b) and c) shows a log-linear plot of S for times $t \geq 1000/N_0$. In all simulations $m_0 = 10k_0$ and $Lk_0 = 0.2$.

During each simulation, we computed the energy above, below and within the staircase, as given by (36). Here we show the results for three simulations, all with $m_0/k = 10$ and $kL = 0.2$ but with different numbers of steps: $J = 2$, 5 and 10. The results are shown in Fig. 6. In all three cases, initially $R = 1$ and $T = S = 0$, corresponding to all the energy lying well above the staircase. As the center of the wavepacket reaches the staircase (in all cases around time $\simeq 1000N_0^{-1}$), the relative energy grows below and within the staircase while decreasing above. At late times the relative energy above and below the staircase plateau to near-constant values as the energy within the staircase decays to zero.

The late-time values of the relative energy below the staircase give the simulated transmission coefficient, which may be compared with the predicted transmission of incident plane waves. This comparison is shown in Fig. 7 for a wide range of simulations, all having $m_0/k = 10$ and with kL spanning a range about the critical transmission wavenumber at $k_cL \simeq 0.2$. The results of simulations for staircases having $J = 1$ and 2 steps are shown in Fig. 7a. Particularly in the case with 1 step, the predicted transmission coefficient corresponds well with the values measured in simulations. In the case of 2 steps, theory moderately under-predicts the measured values for $0.18 \lesssim kL \lesssim 0.25$. In simulations with more steps, the measured transmission versus kL is qualitatively different for the predicted

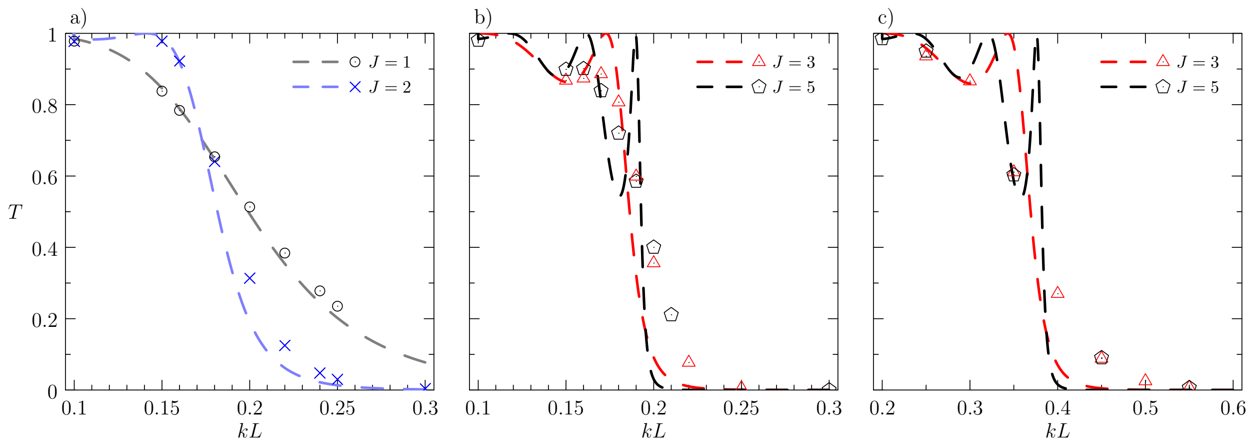

FIG. 7. Measured and predicted transmission as a function of kL in simulations with $m_0 = 10k$ and a) $J = 1$ and 2 steps and b) $J = 3$ and 5 steps, and c) with $m_0 = 5k$ and $J = 3$ and 5 steps. Dashed lines indicate the theoretical prediction for incident plane waves and symbols denote measurements from simulations, as indicated in the legends.

values about $k_c L = 0.2$ (Fig. 7b). The presence of more steps leads to a prediction of more transmission spikes with the highest wavenumber spike having kL close to, but below, $k_c L$. However, the measurements from simulations show a near monotonic decrease in T with increasing kL. In particular, with $J = 5$ and $kL = 0.19$, theory predicts near-perfect transmission, whereas the measured transmission coefficient was 0.59. For the same number of steps but with $kL = 0.20$, theory predicts near-zero transmission, whereas the simulation measured a coefficient of 0.40. Similar behaviour is found in simulations with $m_0 = 5k$ (Fig. 7c) about the critical transmission wavenumber at $k_c L \simeq 0.4$.

A qualitative explanation for the lack of transmission spikes occurring in simulations can be found through closer examination of the time-evolution of relative energy within the staircase, $S(t)$, shown in Fig. 6. In the case with two steps (Fig. 6a), the growth and decay of energy within the staircase is almost symmetric about the peak, which occurs at time $\simeq 1040 N_0^{-1}$. However, in the cases with $J = 5$ and 10 (Figs. 6b,c), the decay of S occurs over a longer time than its initial growth. The insets in Figs. 6b,c) plot $\log_{10}(S)$ versus time, revealing that the late time decay is nearly exponential and the decay is slower with larger J.

By finding a best-fit line through the log plots over times when S falls below a threshold

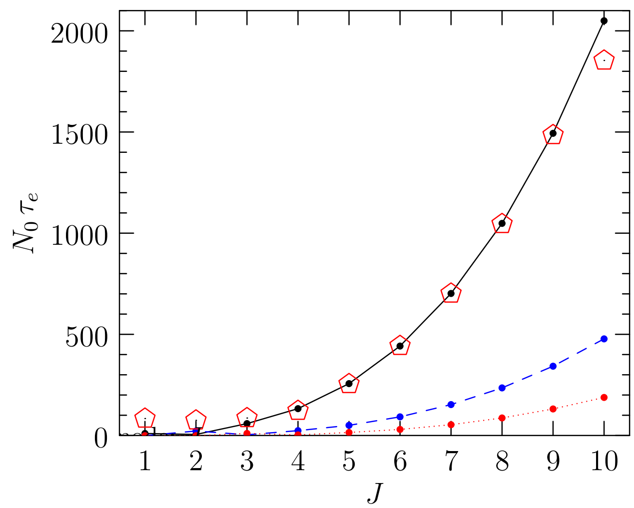

FIG. 8. Effect of the number of steps J on e-folding decay time of energy within the staircase at late times. Open pentagons represent measurements from simulations. The lines denote theoretical predictions based on the energy decay rate of natural modes of the staircase for the highest mode (solid black line), second-highest mode (blue dashed line) and the third-highest mode (red dotted line). In all simulations $A_0 = 0.001\,k_0^{-1}$ and $m_0 = 10\,k_0$, with corresponding frequency $\omega_0 = 0.0995 N_0$.

of 0.01, we measure the exponential decay rate and, from this, get the e-folding energy decay time-scale, τ_e. This is plotted in Fig. 8 for a range of simulations with J ranging from 1 to 10, keeping $m_0 = 10k$ and $kL = 0.2$ fixed. In simulations with $J \geq 4$, τ_e increases rapidly with increasing J. These measured values are compared with the predicted e-folding energy decay time associated with natural modes of the staircase, given by $\tau_j/2$, in which $\tau_j = -1/\omega_j$ where ω_j is the imaginary part of the frequency of mode-j determined from the solution of the eigenvalue problem given by (15). The highest vertical mode has the lowest real and (magnitude of) imaginary frequency and so has the largest predicted e-folding decay time (see Fig. 2b,d). The predicted energy decay times of the highest modes correspond excellently with the measured values, clearly indicating that the incident wavepacket with kL near the critical transition excited the highest vertical mode.

Even after the incident wavepacket partially transmitted and reflected, energy remains in this mode which then continuously transmits waves above and below the staircase as its energy decays. Thus a transmission spike in a 5-step staircase does not occur near $kL = 0.19$ because the incident wavepacket resonated near perfectly with the highest vertical mode of the staircase, which then retransmitted half the absorbed energy as upward propagating waves above the staircase. Likewise, though theory predicts weak transmission for $kL = 0.2$, the measured transmission in simulations is large because half of the incident energy, absorbed in near-resonance with the highest vertical mode, is retransmitted as downward propagating waves below the staircase.

By plotting the results in Fig. 8 on log-log axes and finding a best-fit line to data with $J \geq 4$, we find that the relative energy decay time-scale increases with the number of steps as

$$N_0 \tau_e = (2.09 \pm 0.02) J^3, \tag{37}$$

in which the measured power law exponent, accurate to 0.1%, is consistent with the prediction (17).

V. CONCLUSIONS

We have performed simulations of a quasi-monochromatic wavepacket incident upon a density staircase having a different number of steps, J, and relative step size, kL. In simulations with 1 step, the transmission coefficient from the theory for incident monochromatic waves well-predicted the transmission measured in simulations. However, in simulations with a larger number of steps, the predicted occurrence of transmission spikes near the critical transition wavenumber, $k_c = 2\omega_0/(N_0 L)$, was not evident. Instead the simulations showed a near-monotonic decrease in transmission with increasing kL about $k_c L$. The discrepancy between the theory for monochromatic incident waves and simulations is explained by the near-resonant excitation of the highest vertical mode of the staircase which partially extracts energy from the incident wavepacket and retransmits this energy above and below the staircase as it exponentially decays in time. The measured e-folding decay time of energy corresponded well with the predicted energy decay time for the highest vertical mode.

Due to computational cost, the simulations were necessarily restricted to the study of hydrostatic internal waves uninfluenced by rotation. For example, with $m_0 = 10k$, $\omega_0/N_0 \simeq 0.1$ which is much larger than f/N_0, assuming a typical value of the Coriolis parameter $f \simeq 0.01\, N_0$. In simulations with higher m_0/k and lower ω_0/N_0, the vertical group velocity of the incident wavepacket would have been lower, requiring prohibitively long computational times to simulate the interaction of the wavepacket with the staircase. Nonetheless, the generic nature of our results suggests they can be extended to the inertia gravity wave regime.

Our results indicate that transient effects associated with a wavepacket interacting with a density staircase should be considered if the incident wavenumber is near the critical transition value, k_c. Past theory has shown that k_c well approximates the transition wavenumber even for finite Coriolis parameter f_0 provided $\omega_0 > f_0$ and $kL \ll 1$ [9]. The same study showed that the critical transition wavenumber is relatively insensitive to having steps that vary in size within the staircase about a mean value $\bar{L}$. With these considerations, we tentatively use observations of a density staircase in the Arctic ocean [13] to estimate conditions under which incident waves are near the critical transition. In that study, 20 steps of a staircase were observed between 240 and 290 meters depth, giving a mean step size of $\bar{L} \simeq 2.5\,\mathrm{m}$. The mean buoyancy frequency was observed to be $0.007\,\mathrm{s}^{-1}$ and $f \simeq 1.4 \times 10^4\,\mathrm{s}^{-1}$ at the observed latitude around 78°N. For near-inertial incident waves ($\omega_0 \gtrsim f_0$), the critical transition occurs for $k_c \simeq 0.016\,\mathrm{m}^{-1}$, corresponding to a horizontal wavelength of $\simeq 400\,\mathrm{m}$. It is unlikely that natural processes would create inertia gravity waves with such small horizontal scale. And so our study is more relevant to higher frequency waves that are not significantly influenced by rotation. In particular, for incident waves with relative frequency $\omega_0/N_0 = 0.1$, the critical horizontal wavelength would be $\simeq 80\,\mathrm{m}$. Hence the possible near-resonant excitation of modes in the staircase would occur for internal waves that are excited by a relatively horizontally localized disturbance near the surface, for example by the motion of wind-driven ice floes in the marginal ice zone. Although this may seem restrictive, because the decay time is longer for modes in staircases with more steps the impact of incident waves upon the staircase would persist. For example, in a staircase with $J = 20$ steps, (17) predicts an e-folding energy decay time of $\sim 44\,\mathrm{days}$.

ACKNOWLEDGMENTS

This research was part of the International Research Training Group (ArcTrain) "Processes and impacts of climate change in the North Atlantic Ocean and the Canadian Arctic" (IRTG 1904 ArcTrain), and it was funded by the Deutsche Forschungsgemeinschaft (DFG, German Research Foundation). This paper is a contribution to project W5 of the Collaborative Research Centre TRR 181 "Energy Transfer in Atmosphere and Ocean" (project number 274762653). Partial funding was also provided by the Natural Sciences and Engineering Research Council (NSERC) through their Discovery Grant program.

The authors wish to thank Digital Research Alliance of Canada for providing supercomputing resources and Alain Gervais for helping with code optimization.

Appendix A: Application of interface conditions

From the general formulae for the vertical structure of disturbances in a density staircase with J steps, given by (3), the condition for continuity of the streamfunction across each interface gives the $J+1$ equations

$$\begin{aligned} A_0 + B_0 &= A_1 e^{kL/2} + B_1 e^{-kL/2}, \\ A_j e^{-kL/2} + B_j e^{kL/2} &= A_{j+1} e^{kL/2} + B_{j+1} e^{-kL/2}, \quad j = 1 \ldots J-1, \\ A_{J+1} + B_{J+1} &= A_J e^{-kL/2} + B_J e^{kL/2}. \end{aligned} \tag{A1}$$

The condition for continuous pressure requires continuity of $\hat{\psi}' - (g\bar{\rho}/\rho_0)(k^2/\omega^2)\hat{\psi}$. Applying this at each interface, and using (1) and (A1) gives the $J+1$ equations

$$\begin{aligned} im[A_0 - B_0] &= k[A_1 e^{kL/2} - B_1 e^{-kL/2}] - \tfrac{1}{2} g' \tfrac{k^2}{\omega^2}[A_1 e^{kL/2} + B_1 e^{-kL/2}] \\ k[A_j e^{-kL/2} - B_j e^{kL/2}] &= k[A_{j+1} e^{kL/2} - B_{j+1} e^{-kL/2}] \\ &\quad - g' \tfrac{k^2}{\omega^2}[A_{j+1} e^{kL/2} + B_{j+1} e^{-kL/2}], \quad j = 1 \ldots J-1, \\ im[A_{J+1} - B_{J+1}] &= k[A_J e^{kL/2} - B_J e^{-kL/2}] - \tfrac{1}{2} g' \tfrac{k^2}{\omega^2}[A_J e^{kL/2} + B_J e^{-kL/2}] \end{aligned} \tag{A2}$$

in which $g' = g\Delta\rho/\rho_0 = N_0^2 L$.

These equations can be written in a simpler form by defining the nondimensional variables $\Delta \equiv e^{kL}$, $M \equiv m/k$ and $\Gamma = (1/2)g'k/\omega^2 = kL(M^2+1)/2$. Furthermore, the middle equations (with $j = 1 \ldots J-1$) of (A1) and (A2) are simplified for each j first by eliminating B_j on the right-hand side to give an equation for A_j, and then by eliminating A_j on the right-hand side to give an equation for B_j:

$$\begin{aligned} A_j &= \Delta(1-\Gamma)A_{j+1} - \Gamma B_{j+1} \\ B_j &= \Gamma A_{j+1} - \Delta^{-1}(1+\Gamma)B_{j+1}, \end{aligned} \tag{A3}$$

Appendix B: Approximate dispersion relation for highest mode

Here we find an approximate analytic prediction for the frequency and decay rate of the highest mode in a density staircase, whose frequency is close to the critical transition given by (12), in which we assume $kL \ll 1$. Consequently $|\omega|/N_0 \ll 1$ and $|M| \simeq N_0/|\omega| \gg 1$. At the critical transition $\omega_c/N_0 = kL/2$. And so we expect $\tilde{m} \equiv mL$ $(= MkL) \simeq 2 - \epsilon$ with $|\epsilon| \ll 1$. Thus $\Gamma = kL(M^2+1)/2 \simeq M\tilde{m}/2$.

The implicit relation for the dispersion relation for modes in a staircase is given generally by (15). The value of b_- in this equation is given by (11), which simplifies in the $kL \ll 1$ limit to $b_- \simeq -\Gamma$. Hence (15) can be written as

$$-\Gamma(a_+ + a_-)^2\Lambda_-/b_0 + (a_+^2 - a_-^2)\Lambda_+ \simeq 0. \tag{B1}$$

From the definition of $a_\pm$ in (5), we get the approximate expressions

$$a_+ + a_- \simeq 2 + i\tilde{m} - \tilde{m}^2/2, \quad a_+ - a_- \simeq M(2i - \tilde{m}). \tag{B2}$$

Also using $\tilde{m} = 2 - \epsilon$, (B1) simplifies to

$$(1-\epsilon/2)(2i + (2-i)\epsilon - \epsilon^2/2)\Lambda_-/b_0 + (2 - 2i - \epsilon)\Lambda_+ \simeq 0. \tag{B3}$$

To find approximate expressions for $\Lambda_\pm$, we use the definition of b_+ in (11) with $kL \ll 1$ to get

$$b_+ \simeq 1 - \tilde{m}^2/2 = -1 + 2\epsilon + O(|\epsilon|^2). \tag{B4}$$

Hence, we find

$$b_0^2 \equiv b_+^2 - 1 \simeq -4\epsilon + O(|\epsilon|^2). \tag{B5}$$

In the expressions for $\Lambda_\pm$, we perform a binomial expansion to write (assuming $J \geq 4$)

$$\lambda_\pm^{J-1} = b_+^{J-1} \pm \begin{pmatrix} J-1 \\ 1 \end{pmatrix} b_+^{J-2}b_0 + \begin{pmatrix} J-1 \\ 2 \end{pmatrix} b_+^{J-3}b_0^2 \pm \begin{pmatrix} J-1 \\ 3 \end{pmatrix} b_+^{J-4}b_0^3 + \ldots \tag{B6}$$

Thus we have

$$\Lambda_+ = b_+^{J-1} + (J-1)(J-2)b_+^{J-3}b_0^2/2 + \ldots \simeq (-1)^{J-1}\big[1 - 2(J-1)^2\epsilon\big] + O(|\epsilon|^2), \tag{B7}$$

and

$$\begin{aligned} \Lambda_-/b_0 &= (J-1)b_+^{J-2} + (J-1)(J-2)(J-3)b_+^{J-4}b_0^2/6 + \ldots \\ &\simeq (-1)^{J-1}\big[-(J-1) + (2/3)J(J-1)(J-2)\epsilon\big] + O(|\epsilon|^2). \end{aligned} \tag{B8}$$

Putting these expressions in (B3) and keeping terms up to $O(|\epsilon|)$ gives

$$6(J+i) - [4J^3 + 12iJ^2 - (10+18i)J + (6+9i)]\,\epsilon \simeq 0. \tag{B9}$$

From this we can solve for ϵ, explicitly finding its real and imaginary parts in terms of the number of steps, J. For $J \gg 1$ we find

$$\epsilon \simeq (3/2)J^{-2}\left[1-(7/2)J^{-2}+O(J^{-3})\right]-3iJ^{-3}\left[1-(9/4)J^{-1}-(13/8)J^{-2}+O(J^{-3})\right]. \tag{B10}$$

[1] R. Ferrari and C. Wunsch, Ocean circulation kinetic energy: Reservoirs, sources, and sinks, Ann. Rev. Fluid Mech. **41**, 253 (2009), doi:10.1146/annurev.fluid.40.111406.102139.

[2] B. R. Sutherland, *Internal Gravity Waves* (Cambridge University Press, Cambridge, UK, 2010) p. 378.

[3] E. Kunze, A. J. Williams, and R. W. Schmitt, Optical microstructure in the thermohaline staircase east of Barbados, Deep-Sea Res. **34**, 1697 (1987).

[4] R. W. Schmitt, H. Perkins, J. D. Boyd, and M. C. Stalcup, C-SALT: an investigation of the thermohaline staircase in the western tropical North Atlantic, Deep-Sea Res. **34**, 1697 (1987).

[5] G. Zodiatis and G. P. Gasparini, Thermohaline staircase formations in the Tyrrhenian Sea, Deep-Sea Res. **43**, 655 (1996).

[6] L. Padman and T. M. Dillon, On the horizontal extent of the Canadian Basin thermohaline steps, J. Phys. Oceanogr. **18**, 1458 (1988).

[7] J. D. Guthrie, I. Fer, and J. H. Morison, Thermohaline staircases in the Amundsen Basin: Possible disruption by shear and mixing, J. Geophys. Res. **122**, 7767 (2017).

[8] N. C. Shibley, M.-L. Timmermans, J. R. Carpenter, and J. M. Toole, Spatial variability of the Arctic Ocean's double-diffusive staircase, Oceanography **122**, 980 (2017).

[9] B. R. Sutherland, Internal wave transmission through a thermohaline staircase, Phys. Rev. Fluids **1**, 013701:1 (2016), doi:10.1103/PhysRevFluids.1.013801.

[10] S. Wunsch, Nonlinear harmonic generation by internal waves in a density staircase, Phys. Rev. Fluids **3**, 114803 (2018).

[11] Q. André, A. J. Barker, and S. Mathis, Layered semi-convection and tides in giant planet interiors, Astronomy and Astrophysics **605**, A117 (2017).

[12] L. Rainville, C. M. Lee, and R. A. Woodgate, Impact of wind-driven mixing in the Arctic Ocean, Oceanography **24**, 136 (2011).

[13] M.-L. Timmermans, J. Toole, R. Krishfield, and P. Winsor, Ice-Tethered Profiler observations

of the double-diffusive staircase in the Canada Basin thermocline, J. Geophys. Res. **113**, C00A02 (2008).

[14] S. Boury, R. Supekar, E. C. Fine, R. Musgrave, J. B. Mickett, G. Voet, P. Odier, T. Peacock, J. A. MacKinnon, and M. H. Alford, Observations of double diffusive staircase edges in the Arctic Ocean, J. Geophys. Res. **127**, e2022JC018906 (2022).

[15] B. R. Sutherland and K. Yewchuk, Internal wave tunnelling, J. Fluid Mech. **511**, 125 (2004).

[16] S. Ghaemsaidi, H. V. Dosser, L. Rainville, and T. Peacock, The impact of multiple layering on internal wave transmission, J. Fluid Mech. **789**, 589 (2016).

[17] G. L. Brown and B. R. Sutherland, Internal wave tunnelling through non-uniformly stratified shear flow, Atmos. Ocean **45**, 47 (2007).

[18] J. T. Nault and B. R. Sutherland, Internal wave tunnelling across a mixed region, Phys. Fluids **19**, 016601:1 (2007), doi:10.1063/1.2424791.

[19] M. Mathur and T. Peacock, Internal wave beam propagation in non-uniform stratifications, J. Fluid Mech. **639**, 133 (2009).

[20] K. Gregory and B. R. Sutherland, Transmission and reflection of internal wave beams, Phys. Fluids **22**, 106601 (2010), doi:10.1063/1.3486613.

[21] G. L. Brown, A. B. G. Bush, and B. R. Sutherland, Beyond ray tracing for internal waves. Part II: Finite-amplitude effects, Phys. Fluids **20**, 106602:1 (2008), doi:10.1063/1.2993168.

[22] M. A. Belyaev, E. Quataert, and J. Fuller, The properties of g-modes in layered semiconvection, MNRAS **452**, 2700 (2015).

[23] B. R. Sutherland and H. Yassin, The nonlinear evolution of internal tides. Part 2: Lagrangian transport by periodic and modulated waves, J. Fluid Mech. **948**, A22 (2022).